Vibration Characteristics of Laminated Composite Plates with Embedded Shape Memory Alloys

Run-xin Zhang [a], Qing-Qing Ni *[b], Arata Masuda [c],

Takahiko Yamamura [c], Masuharu Iwamoto [a]

[a] Division of Advanced Fibro-Science, Kyoto Institute of Technology, Matsugasaki Sakyo-ku, Kyoto 606-8585, Japan

*[b] Dept. of Functional Machinery and Mechanics, Shinshu University, 3-15-1 Tokida, Ueda 386-8567, Japan

[c] Department of Mechanical and System Engineering, Kyoto Institute of Technology, Matsugasaki Sakyo-ku, Kyoto 606-8585, Japan

* *Corresponding author*

E-mail: niqq@shinshu-u.ac.jp

Fax: +81-268-215438

Tel: +81-268-215438

ABSTRACT

Shape memory alloy (SMA) is commercially available for a variety of actuator and damping materials. Recently, SMA wires have also become commercially available for the design of smart composite structures because SMA wires with a small diameter can be easily produced. In this work, two types of SMA-based composites are presented for investigating the vibration characteristics. First, laminated composite plates containing unidirectional fine SMA wires are fabricated. By measuring the vibration mode of a clamped cantilever, the influence of both SMA arrangement and temperature on the vibration characteristics is made clear. Next, laminated composite plates with embedded woven SMA layer are fabricated. The stiffness tuning capability is evaluated by impact vibration tests with different temperatures. It is found that the stiffness tuning capability may be improved by increasing the volume fraction of SMAs and by controlling accurately the internal stress according to the phase transformation temperature of SMAs from martensite to austenite. The theoretical prediction on the natural frequency considering the SMAs behavior and laminated structures is proposed and their results agree reasonably with experimental ones.

.

Key Words: Shape memory alloy; Composites; Weaving; Vibration property

1. INTRODUCTION

Textile reinforced composites made of resin-infiltrated textile with various architectures, such as 2D/3D woven fabric, 2D/3D braiding, knitting and stitching, have attracted growing interest due to their excellent potential of shape forming, light weight, and other attractive mechanical properties. Prepregs made of woven glass or carbon fibers, for example, are well standardized and widely used for making easily both light and tough structures. One of the most challenging and comprehensive projects of applying the advanced textile composites to more complex structures, such as wings and fuselages, has been reported by NASA [1].

Shape memory alloys (SMAs) have unique mechanical and thermodynamic properties such as shape memory effect and pseudoelasticity. They have been used as "smart" components embedded into the conventional resins or composites so as to obtain active abilities, including in tunable stiffness, damping capacity, shape-controllable active surfaces and self-healing capability. Many works have been done and shown that SMAs have significant potential applications for vibration control and structural control [2-8]. Although two-dimension weaving metal wires, such as stainless wires, are common in industry applications, to the authors' knowledge, a preliminary study of weaving SMA wires has been reported by Boussu et al. [7]. They made the woven SMA fabric using NiTi thin wires with 0.15 mm diameter. Unfortunately, the practical detail of the fabrication is not disclosed. At present, the fabrication process of textile SMA-based composites are still complicated and non-standardization.

SMAs used as reinforcements or actuators in composite materials can be of numerous structural designs because their parameters are available in unique control. The textile composites with smart SMA-based seems to be quite promising since the tremendous diversity of textile architecture allows the SMA components to easily fabricate their various forms. For example, SMA wires or yarns can be used as "smart fibers" combined with

conventional glass/carbon fibers so as to make a part of the textile perform multi-functional properties. Moreover, if one introduces SMA fibers into a braided stent, it may be used as an active probe. The concept may lead to more stable and handier fabrication process for the SMA-based smart composites, just as woven glass/carbon fiber prepregs have made the fabrication of GFRP/CFRP structures much easier.

In the present study, two types of SMA-based composites were fabricated and their mechanical properties, especially for natural frequency as a function of temperature, were investigated. First, the laminated composite plates containing unidirectional fine SMA wires are fabricated. By measuring the vibration mode of a clamped cantilever, the influences of both SMA arrangements and temperatures on the vibration characteristics of the laminated plates are discussed and simulated. Next, the SMA-based textile laminated composites are fabricated by weaving techniques. The stiffness tuning capability of the laminated plates with SMAs is evaluated by impact vibration tests. Since the SMA wires are expected to give the laminated plate multi-functions such as active actuation, tunable stiffness and damping capacity, the vibration characteristics of the developed SMAs is investigated based on laminated composite plates below and above the phase transformation temperature from martensite to austenite.

2. EXPERMENTAL PROCEDURES

2.1 Materials

The SMA wires in the present study were linearly memorized martensitic Ti-Ni alloy (KIOKALLOY-R) produced by Daido Steel Co., Ltd. Japan. The diameters of SMAs were 0.2 and 0.4 mm. The phase transformation temperature for austenite of the Ti-Ni alloy is about 55ºC. The polymer material used as a matrix was the ER3 epoxy resin, and the hardening agent was EH208W produced by PLUS PLAGKS Co., Ltd., Japan. The resin had a high impact resistance property, and the glass transition temperature (T_g) was approximately

140 ºC. The variation of the elastic modulus with temperature for ER3 epoxy resin was measured, as shown in Fig. 1. Cross-ply CFRP used in this study was produced by Mitsubishi Rayon Pyrofil. The engineering constants of the Ti-Ni alloy and the other materials were listed in Table 1.

2.2 Specimen fabrication

ER3 epoxy resin was dried for 20 min by a vacuum bump. After then, the resin was poured into a model and cured at room temperature for 24 hours. Further, the molding was moved to a heating oven and heated from 40ºC to 140ºC at a rate of 10ºC per hour. As shown in Fig. 2, the resin bulk plate and three kinds of the laminated composite plates with embedded unidirectional SMA were fabricated. No. 2 specimen had 5 SMA wires of 0.2 mm in diameter and a fraction of 0.44 vol%. Nos. 3 and 4 specimens had 5 and 17 SMA wires of 0.4 mm in diameter, and SMA volume fractions of 1.57 % and 5.35 %, respectively. The dimension of beam used in this test was 250×20×2.2 mm.

In the present study, the weaving SMA meshes were performed by hand-made. We first tried to utilize hand-weaving machine since an appropriate weaving machine was not available, but the process failed because it was quite difficult to keep the quality of the weft such as tension and equal pitch, etc. Thus, an apparatus shown in Fig. 3 was developed to align the SMA wires and to maintain proper geometries and restraints on the warp and weft wires. Fig. 4 shows the type of the SMA meshes with a plain weaving structure. The SMA wires were a diameter of 0.2 mm and had a pitches of p_1=p_2=2 mm.

Strain control was the most important and difficult in preparing SMA actuators. The SMA wires were heated frequently in the weaving process so as to eliminate the packaging stress and strain due to bending and twisting deformation produced by the weaving operation. After weaving, the warp and weft were slightly pulled using the apparatus to remove the slack from

the woven mesh. The schematic illustrations of three specimens fabricated in this study are shown in Fig. 5.

No.1 specimen was an epoxy plate sandwiched between two carbon cloth (CC) preprags with plain texture. The stack sequence of the plate was [CC/epoxy/CC]. No.2 specimen had a woven steel mesh (d=0.2 mm, p_1=p_2=1.25 mm) embedded between the carbon cloth and the epoxy resin layer. The stack sequence was [CC/steel/epoxy/CC]. No.3 specimen had woven SMA mesh embedded between the carbon cloth and the epoxy layer. The lamination was represented as [CC/SMA/epoxy/CC]. First, the epoxy resin plates with 1 mm thickness were fabricated without aftercure process. Then, the lamination of the epoxy plate, the carbon cloth prepregs and the SMA mesh (or the steel mesh) was assembled on a tooling plate. The entire assembly was vacuumized, and subjected to a cure process for 2 hours with a hot press of 130ºC and 690 MPa. Following an oven cure, the laminated plates used for test were machine-tooled to make rectangular plates with a dimension 150×250 mm. The overall fractions of the SMA and the steel are approximately 1.2 and 2.4 vol%, respectively.

2.3 Experiment

The specimens were first heated up to 130ºC using a heating furnace, and then clamped in the form of cantilever beams with 180 mm span. The beam was vibrated by Rion vibrator with a frequency of 100 Hz when it was freely cooled down. The surface temperature on the specimens was measured with the thermo tracer TH3100 (NEC mishi ei Co., Ltd.). A acceleration sensor (CF-350), AD converter and computer were used to measure the natural frequency of the beams. The schematic illustration of the experimental setup for the vibration testing is shown in Fig. 6. In terms of Fourier transformation, the vibration characteristics were obtained from damping waveforms measured.

For the laminated composite plates with embedded woven SMAs, the specimens were

clamped on a steel fixture as shown in Fig. 7(a). The effective dimensions of the plates, which can be vibrated in the fixture, were 120×236 mm.

Before measurement for the vibration characteristic, all of the specimens were subjected to temperature cycles from room temperature to 120ºC so as to make them stability in thermodynamic property. Next, the specimens were once heated up to 120ºC on the furnace, then taken out and measured immediately at room temperature. The vibration of laminated plates was measured by accelerometers attached to the specimens, as shown in Fig. 7(b). After the specimens were excited with a hammer, the transient vibration response was obtained to evaluate the natural frequency of the laminated plates. The impact-measurement cycle was repeated many times until the surface temperature on specimens was settled down room temperature. The surface temperature of specimens was measured by an infrared camera set shown in Fig. 7(b).

2.4 Analysis of vibration

For a simple elastic beam problem with uniform cross-sectional area, a well-known natural frequency can be given by [9]

$$f = \frac{\beta^2}{2\pi l}\sqrt{\frac{EI}{S\rho}} \tag{1}$$

where S and l are the cross-section and the length of the laminated composite beam, respectively. β is a constant relative to the vibration bound condition. In a cantilever beam, β is equal to 1.875 for the first mode of vibration. ρ is the density of the laminated beam. EI is the equivalent bending stiffness. Using the concept of classical composite-beam theory, the equivalent bending stiffness of the laminated beam can be easily approximated as given in Appendix A. Moreover, the stiffness of a lamina composed of a resin and embedded discrete SMA fibers can be given by the rule of mixtures.

For a plate with special orthotropy, the governing differential equation of motion can be

given by [10]

$$D_{11}\frac{\partial^4 w}{\partial x^4}+2\left(D_{12}+2D_{66}\right)\frac{\partial^4 w}{\partial x^2\partial y^2}+D_{22}\frac{\partial^4 w}{\partial y^4}+\rho h\frac{\partial^2 w}{\partial t^2}=0 \tag{2}$$

where h is the thickness of the laminated composite plates.

In order to obtain the solution of the vibration frequency, Rayleigh-Ritz method can be used to solve above differential equation. In the present analysis, the vibration testing can be considered approximately to be simply supported boundary condition because only very narrow sides of the laminated plates were fixed to the frame (Fig. 8). Therefore, the amplitude of the transverse displacement of the plate can be express by the separation of variables:

$$w=C_{mn}\sin\frac{m\pi x}{a}\sin\frac{n\pi y}{b}e^{i\omega t} \tag{3}$$

where m and n are equal to 1 for the lowest vibrational mode of plates. a and b are the side length of a plate.

Substituting Eq. (3) into (2), we have

$$\omega_{mn}=\frac{\pi^2}{\sqrt{\rho h}}\sqrt{D_{11}\left(\frac{m}{a}\right)^4+2\left(D_{12}+2D_{66}\right)\left(\frac{m}{a}\right)^2\left(\frac{n}{b}\right)^2+D_{22}\left(\frac{n}{b}\right)^4} \tag{4}$$

The equivalent bending stiffness of the laminated plate, $D_{ij}\ \left(ij=11,22,12,66\right)$, are estimated closely by means of the general lamination theory as given in Appendix.

3. RESULTS AND DISSCUSSIONS

3. 1 Unidirectional SMA laminated composite beams

3.1.1. Temerature dependency of natural frequency

Fig. 9 shows the variation of the natural frequency for the laminated beams with embedded SMAs at elevated temperature. Since epoxy resin (No.1 specimen) exhibits low stiffness at high temperature, increasing temperature results in lower vibration frequency. Except for the No.4 specimen, the natural frequency of all the beams decreases with

increasing temperature. This is because the laminated composite beams filled with lower SMA fraction will have their mechanical behavior mainly depending on the properties of the resin matrix with lower stiffness at high temperature. For the No.4 specimen, the natural frequency of vibration also decreases with increasing temperature within the martensitic phase of the SMA wire and the beam has the increasing natural frequency in austenitic phase after heating to above 50ºC. So, an obvious concave point on the curve of natural frequency vs. temperature is observed, which is just near the phase transformation temperature of austenite phase. The No.4 specimen around 80ºC is up to the highest natural frequency, and then decreases with an increase in temperature. This is because the elastic modulus of the resin matrix decreases rapidly when the temperature is above 80ºC. However, the total curves of natural frequency vs. temperature for these four specimens moved to higher natural frequency side when the SMA fraction is increased, i.e., the natural frequency at each temperature increased with increasing SMA fraction. At the same time, the changes of the curvature near the austenite phase transform temperature on the curves of natural frequency vs. temperature is observed for Nos. 2, 3, 4 with SMA wires embedded, and it becomes obvious with the increment of SMA fraction. This means that the SMA wires embedded in laminated composite plates play an initiative role in increasing natural frequency of the composite beam.

To clarify the effect of SMA wires in above specimens, the data in Fig. 9 normalized by the epoxy resin specimen (the No. 1 specimen) are shown in Fig. 10. It is obvious that the effect of SMA wires embedded in the composite plate on the natural frequency is significant. For the No. 4 specimen, the natural frequency increases to twice times at a temperature of about 100ºC compared to the resin beam. This result shows that the damping controls by using SMAs should be possible.

According to equation (1) and the Appendix A, on the other hand, a theoretical prediction on natural frequency as shown in Fig. 11 can be calculated. For all of the specimens, although

the predicted results are little smaller than the experimental ones, the temperature dependency of the natural frequency (see the shape of curves) for theoretical prediction agrees reasonably with the experimental results.

3.1.2. Damping behavior

A beneficial characterization of the SMA wires is their good damping property at super-elastic status. Several damping parameters, such as inner fraction, loss factor and loss tangent $\tan\delta$ [9] have been used individually or combined for metals, ceramics, and rubbers, according to the material properties and test methods. For the present materials with SMA wires, the logarithm attenuation coefficient is used, which can be evaluated by measuring the vibration amplitude during the experiment. A classical damping equation for vibration beams is expressed in the form of

$$\Delta = \ln\left(x_n / x_{n+1}\right) \tag{5}$$

where x_n, x_{n+1} are the amplification of sine wave with logarithm damping in different interval, as shown in Fig.12. Moreover, $\Delta = \pi\eta$, is used commonly to determine the damping coefficient η.

Fig. 13 shows the damping effects of the vibration beam at elevated temperature. At the temperature below 50ºC, the SMA laminated beams exhibit a slightly larger logarithm attenuation coefficient than the beam of the epoxy resin (No.1). Since the epoxy resin transfers to rubbery state with increasing temperature, the logarithm attenuation coefficient of the resin beam rises rapidly when the resin matrix becomes high viscoelastic behavior. The logarithm attenuation coefficient of the SMA laminated beams increases with increasing volume fraction of the SMA wires. For the No.4 specimen with larger SMA volume fraction, the logarithm attenuation coefficient of the beam is the largest before the austenite phase transform temperature. Because the stiffness of the SMA wires inside the laminated composite

beam increases with increasing temperature, the laminated beam shows low vibration resistance under higher temperature. For another SMA laminated beams (No.2 and 3), the logarithm attenuation coefficient increases slightly following the phase transformation temperature, but tends to increase rapidly after the temperature above 80ºC. The reason is that the stiffness of the resin matrix of the laminated beams decreases rapidly when heated to high temperature. On the other hand, the volume fraction of the SMA wires is too small to raise the overall stiffness of the laminated composites. These results represent that the use of SMA wires is able to valuably improve the damping properties of composite beams and control their vibrational frequency.

3. 2 Woven SMA laminated plates

For the laminated plate with two-dimensional boundary conditions, the natural frequency of vibration with the lowest mode could be identified by Fourier transform of the waveforms of the transient response of specimens in the experiments as shown in the previous measuring system (see Fig. 7). The experimental results on the natural frequency are shown in Fig. 14. It is shown from Fig. 14 that the natural frequency of the No.1 specimen decreases slightly with increasing temperature, which can be considered as the result of temperature dependency of epoxy resin due to the softening of the epoxy resin (see Fig. 1). At room temperature, the natural frequencies in the No.2 or No.3 specimens are much higher than that of the No.1 specimen due to the embedded steel or SMA meshes with high modulus. However, the natural frequency of No.2 specimen with the steel mesh falls down obviously as temperature is increased. At high temperature, the natural frequency of vibration may become close to that of the No.1 specimen without steel mesh. This result suggests that the interfacial strength may become very low (almost zero) and the debonding region may exist between the steel mesh and the epoxy resin due to elevated temperature, and thus the steel mesh lose their

reinforcement effect in the laminated plates. At room temperature, the natural frequency of vibration for the No.3 specimen is approximately equal to that for the No.1 specimen of epoxy resin. The natural frequency of the No.3 remains nearly constant up to 100ºC in contrast to the stiffness dropping observed in the Nos.1 and 2 specimens. This can be explained as that the hardening effect of austenitic phase transformation will start around 55 ～60ºC and the consequence of high stiffness in SMAs with austenite at elevated temperature will contribute the high natural frequency for this specimen even at the temperature over 55ºC.

In order to compare the effect of SMAs mesh in above specimens, the data in Fig. 14 normalized by the epoxy resin specimen (the No. 1 specimen) are shown in Fig. 15. It is obvious that the effect of SMA wires embedded in the composite plate on the natural frequency is large. For the No. 3 specimen, the natural frequency increases to about 1.8 times at any temperature when compared with the resin beam. The results indicate that the damping control using SMAs mesh is an effective way to practical use.

According to the previous Eq. (4) and Appendix B, the theoretical prediction of the natural frequency under the four simply supported edges for the three specimens is shown in Fig. 15. The predicted results are smaller than those in experiments. The reason for this difference is mainly that in the experiments the practical edge condition as shown in Fig. 8 is not a perfect one like simply supported conditions. The pretension of woven SMA mesh was not perfectly controlled so that the geometry of SMA mesh may have been altered, such as wound, twisted or kinked, when they were embedded to laminated composite plates. For more accurate prediction of the natural frequency, it seems also necessary to take into account of the crimp and the mutual connection between woven SMA wires.

However, the theoretical prediction in Fig. 16 shows some reasonable results that are comparable with the experimental ones. The natural frequency of vibration for the Nos. 2 and

3 specimens is approximately two times larger than that for the No.1 specimen of epoxy resin. The natural frequency in the No.3 specimen increases when the temperature is over 55ºC due to austenite of SMAs, and the curve of natural frequency vs. temperature shows a variation on natural frequency near the austenite phase transformation temperature. With above observations, the predicted temperature dependency of the natural frequency for three specimens is reasonable. Although the difference between theoretical prediction (Fig. 16) and experimental results (Fig. 14) is observed from temperature dependency of the natural frequency (especially for the No.2 specimen), this may mainly resulted from the debonding failure and the reduction of interfacial strength in practical specimens as mentioned previously, which were not token into account in the theoretical prediction in this study. Thus, it is clear that the laminated composite plates with woven SMAs mesh will possess high natural frequency especially at an elevated temperature, and this also shows a possible way for damping control in practical material structures by using woven SMAs.

4. CONCOULSIONS

Two types of laminated composite plates with unidirectional and woven SMAs are fabricated and their vibration characteristics are investigated by both impact vibration tests and theoretical analysis.

For the composite beams with embedded SMA wires, the change in the vibration properties is less significant at low temperatures, but it is sensitive at high temperatures due to the austenite phase transformation. The natural frequency of the laminated beams increases with increasing volume fraction of SMA wires. The natural frequency in the SMA laminated beam with only about 5% volume fraction of SMAs is almost two times larger than that in the epoxy resin at the austenite phase transformation temperature A_f. The SMAs contribution on the natural frequency in composite plates is confirmed. For the woven SMA laminated

composite plates, it is clear that the developed laminates possess high natural frequency especially at an elevated temperature.

According to the present results, it can be expected that the vibration and damping properties can be improved by designing the SMA laminated structures with proper volume fraction of SMA wires and controlling their prestrain more accurately during molding process. The theoretical model analysis proposed in this work is simple, but the predicted results on the natural frequency of vibration agree reasonably with the experimental measurement. Both experiment and analysis indicate that using SMA wires or woven SMAs mesh should be an effective way to damping control in practical material structures.

ACKNOWLEDGMENT

The authors would like to express their appreciation to Mr. Sawayi for the cooperation on preparing experimental apparatus.

Appendix A

The equivalent bending stiffness *EI* obtained according the classical composite-beam theory can be given as

$$EI = \frac{E_c b D^3}{12} + \frac{E_m b\left(h^3 - D^3\right)}{12} \qquad \text{(No. 2 and No. 3)} \tag{A1}$$

$$EI = \frac{2E_c b}{3}\left[\left(\frac{h+4D}{6}\right)^3 - \left(\frac{h-2D}{6}\right)^3\right] + \frac{2E_m b}{3}\left[\frac{h^3}{8} + \left(\frac{h-2D}{6}\right)^3 - \left(\frac{h+4D}{6}\right)^3\right] \quad \text{(No. 4)} \tag{A2}$$

where *b* and *h* is the width and thickness of a plate, respectively. *D* is the diameter of SMA wires. E_m is the elastic modulus of epoxy resin. E_c is the elastic modulus of a lamina composed of a resin and embedded SMA fibers. The lamina thickness is considered to be the diameter of SMA wires, thus the elastic modulus of the composite lamina can be given by the rule of mixtures:

$$E_c = E_{SMA} V_{SMA} + E_m\left(1 - V_{SMA}\right) \tag{A3}$$

where E_{SMA} and V_{SMA} are the elastic modulus and the volume fraction of the SMAs relative to the lamina, respectively.

Appendix B

Fig. 17 shows the model for a lamina made of a matrix sheet with cross-ply SMA fibers embedded. The effective stiffness of the lamina can be expressed as follows:

$$Q_{11} = \frac{1}{2}\left(\frac{E_{X1}}{1-\upsilon_{XY1}\upsilon_{YX1}} + \frac{E_{X2}}{1-\upsilon_{XY2}\upsilon_{YX2}}\right), \tag{B1}$$

$$Q_{22} = \frac{1}{2}\left(\frac{E_{Y1}}{1-\upsilon_{XY1}\upsilon_{YX1}} + \frac{E_{Y2}}{1-\upsilon_{XY2}\upsilon_{YX2}}\right), \tag{B2}$$

$$Q_{12} = \frac{1}{2}\left(\frac{\upsilon_{XY1}E_{Y1}}{1-\upsilon_{XY1}\upsilon_{YX1}} + \frac{\upsilon_{XY2}E_{Y2}}{1-\upsilon_{XY2}\upsilon_{YX2}}\right), \tag{B3}$$

$$Q_{66} = \frac{1}{2}\left(\frac{G_f G_m}{G_m V_f^1 + G_f\left(1-V_f^1\right)} + \frac{G_f G_m}{G_m V_f^2 + G_f\left(1-V_f^2\right)}\right), \tag{B4}$$

where

$$E_{X1} = E_{SMA}V_{SMA}^{1} + E_m\left(1 - V_{SMA}^{1}\right), \qquad E_{Y1} = \frac{E_{SMA}E_m}{E_{SMA}\left(1 - V_{SMA}^{1}\right) + V_{SMA}^{1}E_m}, \tag{B5}$$

$$E_{X2} = \frac{E_{SMA}E_m}{E_{SMA}\left(1 - V_{SMA}^{2}\right) + E_m V_{SMA}^{2}}, \qquad E_{Y2} = E_{SMA}V_{SMA}^{2} + E_m\left(1 - V_{SMA}^{2}\right), \tag{B6}$$

$$\upsilon_{XY1} = \upsilon_{SMA}V_{SMA}^{1} + \upsilon_m\left(1 - V_{SMA}^{1}\right), \qquad \upsilon_{XY2} = \upsilon_{SMA}V_{SMA}^{2} + \upsilon_m\left(1 - V_{SMA}^{2}\right), \tag{B7}$$

$$\frac{\upsilon_{XY1}}{E_{X1}} = \frac{\upsilon_{YX1}}{E_{Y1}}, \qquad \frac{\upsilon_{YX2}}{E_{Y2}} = \frac{\upsilon_{XY2}}{E_{X2}}. \tag{B8}$$

Using the classical lamination theory, the equivalent bending stiffness, D_{ij} , can be estimated by

$$D_{ij} = \sum_{k=1}^{n} \eta_k \left(Q_{ij}\right)_k, \qquad (ij = 11, 22, 12, 66). \tag{B9}$$

where η_k is a constant dependent on the geometry of the lamination. $\left(Q_{ij}\right)_k$ is the stiffness at *k*th layer.

REFERENCES

[1] Dow M.B., Dexter H.B., Development of stitched, braided and woven composite structures in the ACT program and at Langley Research Center (1985 to 1997): summary and bibliography. NASA/TP-97-206234, 1997.

[2] Turner T.L., Patel H.D., Analysis of SMA hybrid composite structures using commercial codes. Proc. SPIE 2004;5383:12.

[3] Xu Y., Otsuka K., Yoshida H., Nagai H., Oishi R., Horikawa H., Kishi T., A new method for fabricating SMA/CFRP smart hybrid composites. Intermetallics 2002;10:361-9.

[4] Ostachowicz W.M., Kaczmarczyk S., Vibration of composite plates with SMA fibers in a gas stream with defects of the type of delamination. Comp Struc 2001;54:305-11.

[5] Baz A., Imam K., McCoy J., Active vibration control of flexible beams using shape memory actuators, Journal of sound and vibration. 1990;140:437-56.

[6] Turner T.L., Lach C.L., Cano R.J., Fabrication and characterization of SMA hybrid composites, Porc SPIE 2001;4333:60.

[7] Boussu F., Bailleul G., Petitniot J.L., Vinchon H., Development of shape memory alloy fabrics for composite structures, AUTEX Research Journal 2002;2:1–7.

[8] Turner T.L., Structural acoustic response of a shape memory alloy hybrid composite panel, Proc SPIE 2002;4701:592–603.

[9] Dym C.L., Shames I.H., Solid mechanics: A vibrational approach. New York, McGraw-Hill, 1973.

[10] Whitney J.M., Structural analysis of laminated anisotropic plates. Lancaster, Technomic Pub. Co., 1987.

Table and Figure Captions

Figure 1

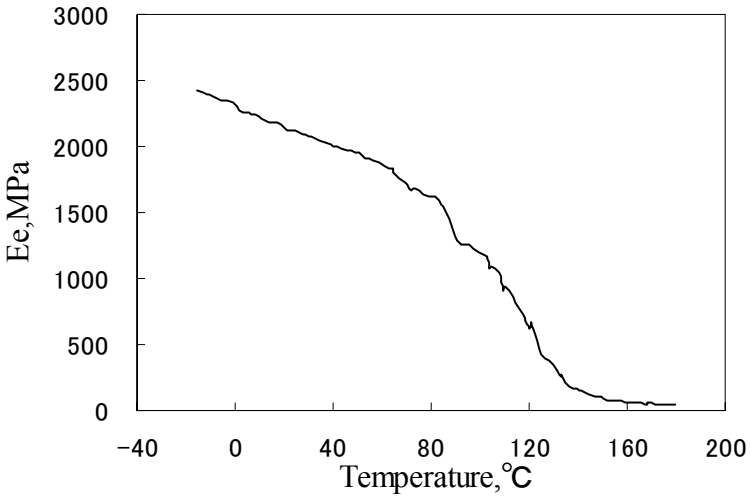
3000
2500
2000
1500
1000
500
0
Ee,MPa
−40
0
40
80
120
160
200
Temperature,℃

Figure 2

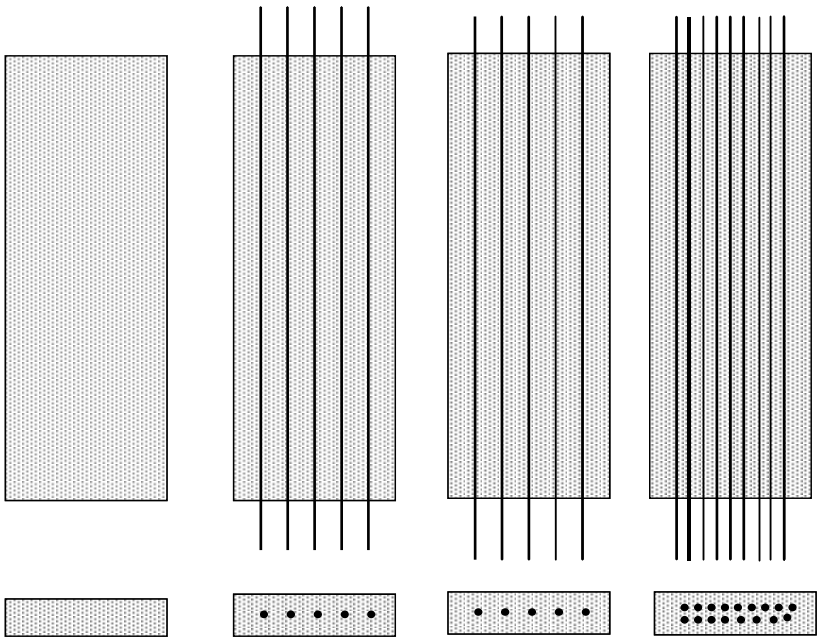

Figure 3

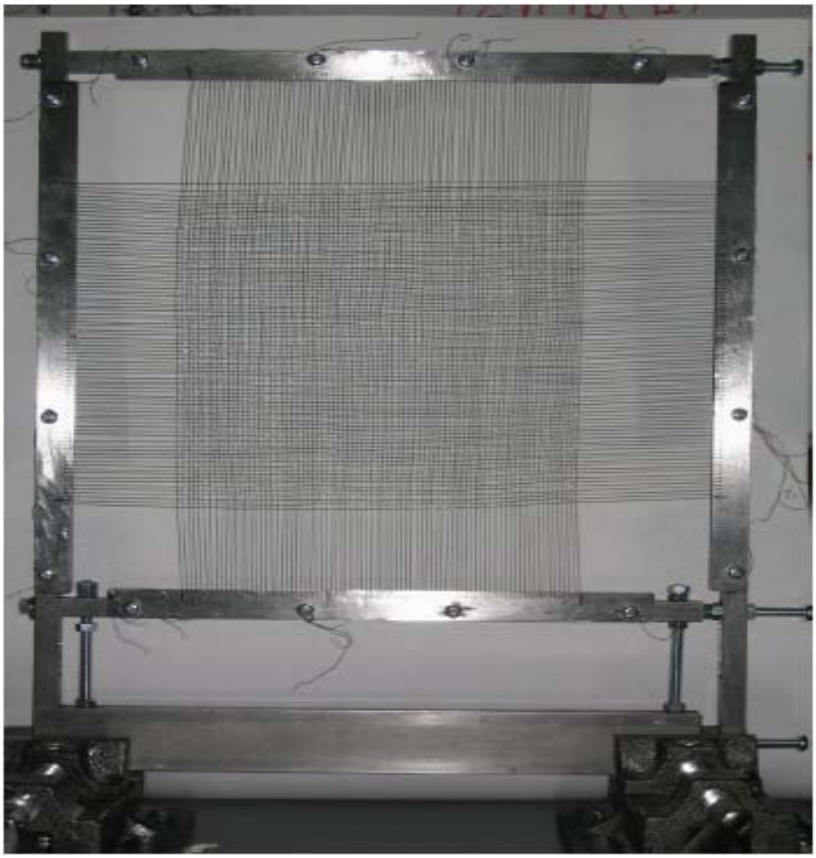

Figure 4

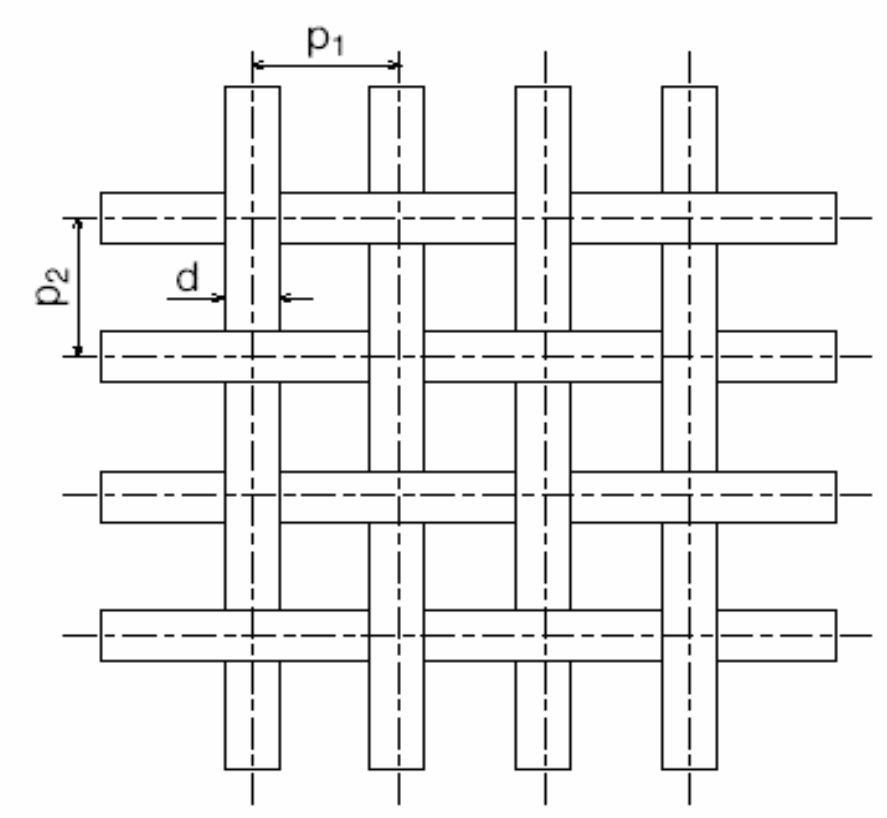

Figure 5

(a) No.1: CC/epoxy/CC (Thickness=1.4 mm)

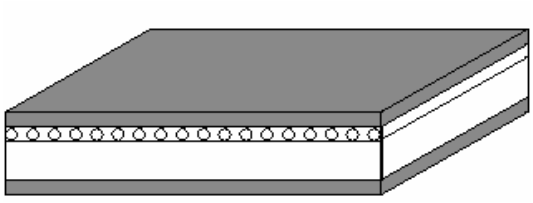

(b) No.2: CC/steel/epoxy/CC (Thickness=2.1 mm)

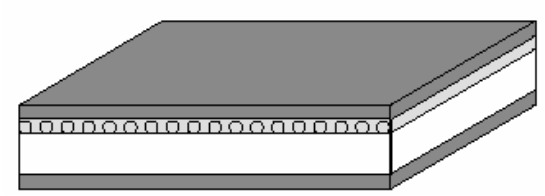

(c) No.3: CC/SMA/steel/epoxy/CC (Thickness=2.1 mm)

Figure 6

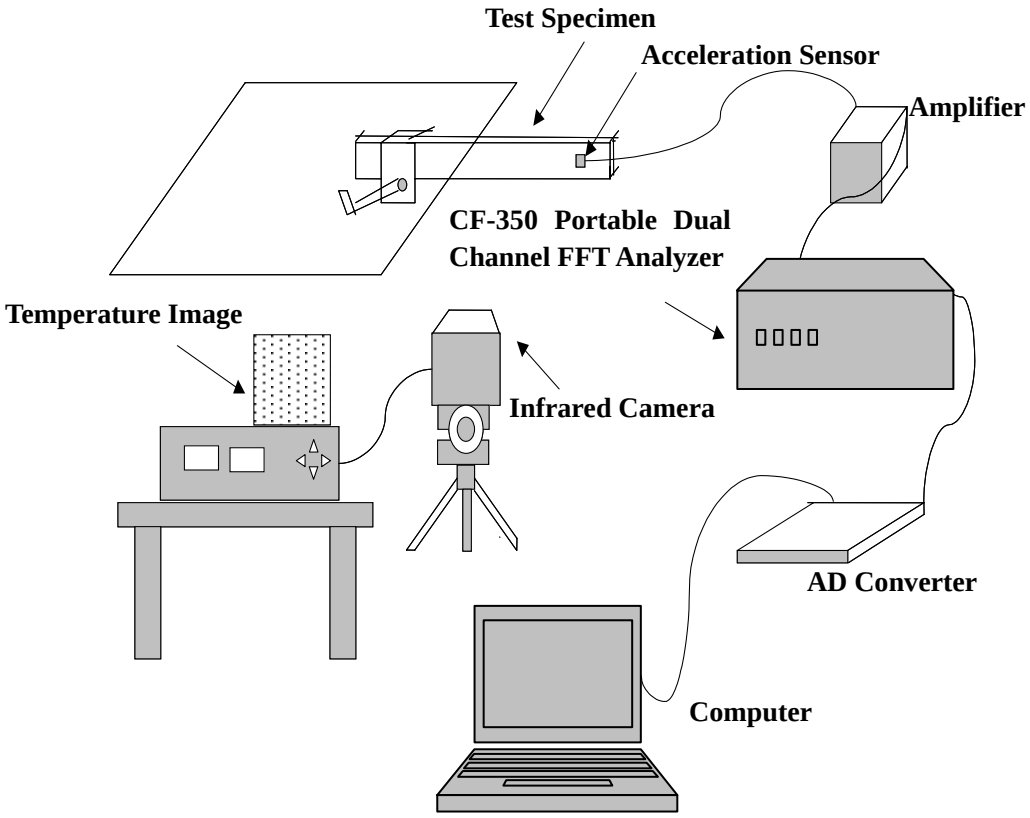
Test Specimen
Acceleration Sensor
Amplifier
CF-350 Portable Dual
Channel FFT Analyzer
Temperature Image
Infrared Camera
AD Converter
Computer

Figure 7

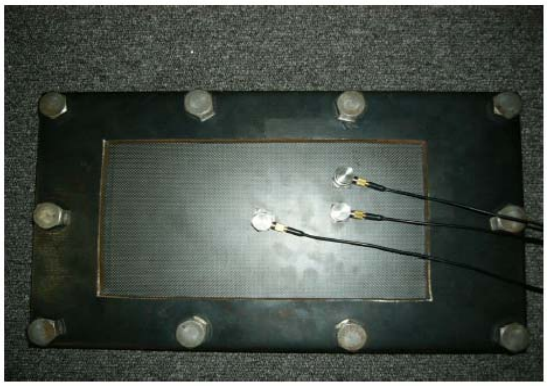

(a) Composite plate with sensors supported in the fixture

(b) Overview

Figure 8

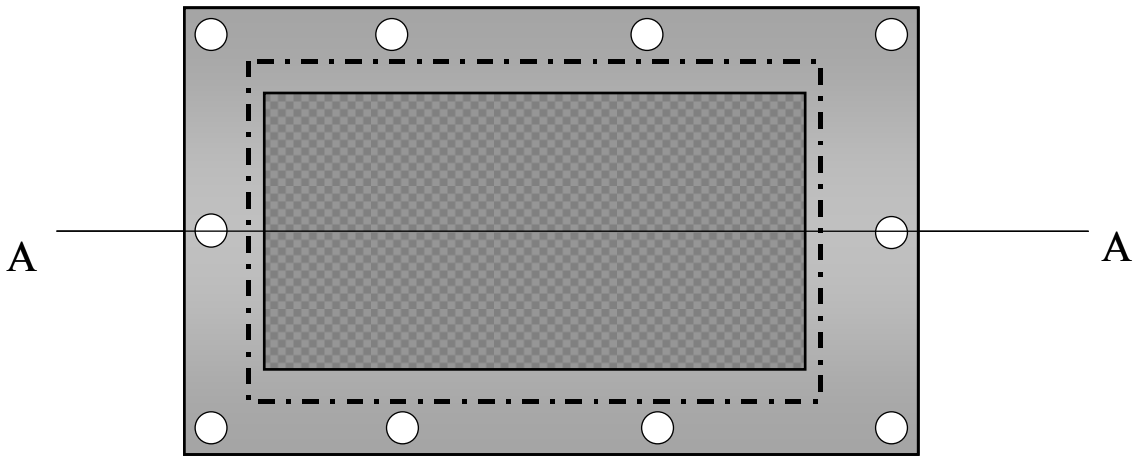

A-A

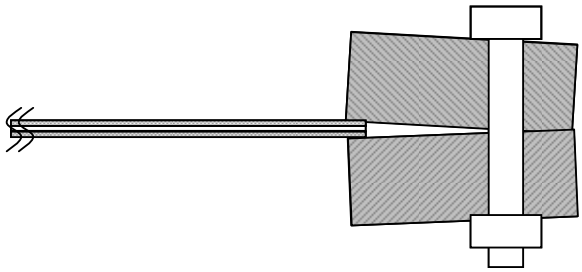

Figure 9

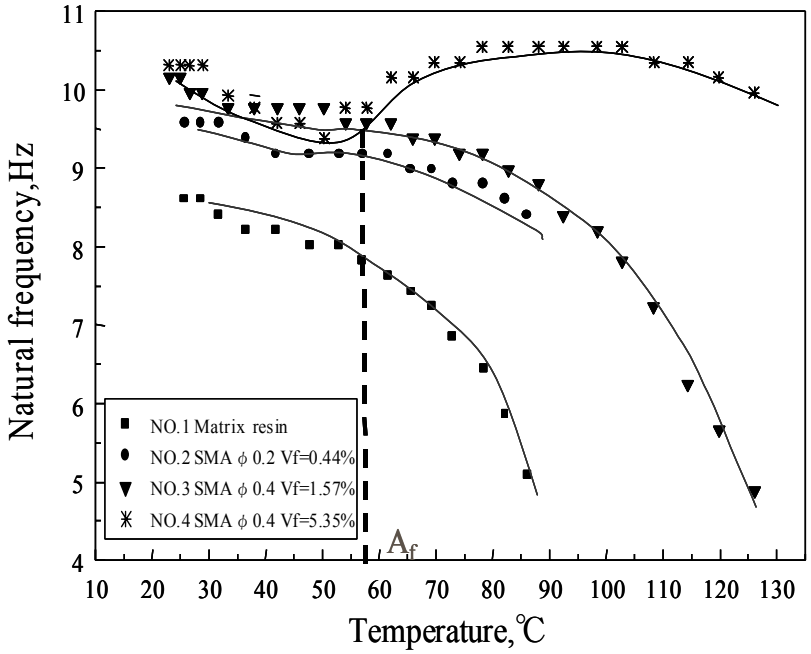
Natural frequency,Hz
Temperature,℃
NO.1 Matrix resin
NO.2 SMA φ 0.2 Vf=0.44%
NO.3 SMA φ 0.4 Vf=1.57%
NO.4 SMA φ 0.4 Vf=5.35%
A_f

Figure 10

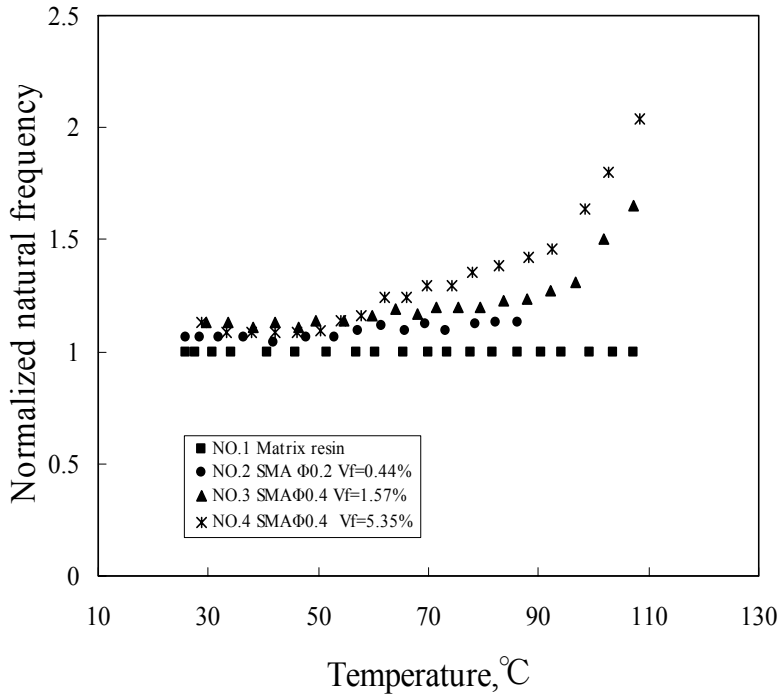
Normalized natural frequency
Temperature,℃
2.5
2
1.5
1
0.5
0
10
30
50
70
90
110
130
NO.1 Matrix resin
NO.2 SMA Φ0.2 Vf=0.44%
NO.3 SMAΦ0.4 Vf=1.57%
NO.4 SMAΦ0.4 Vf=5.35%

Figure 11

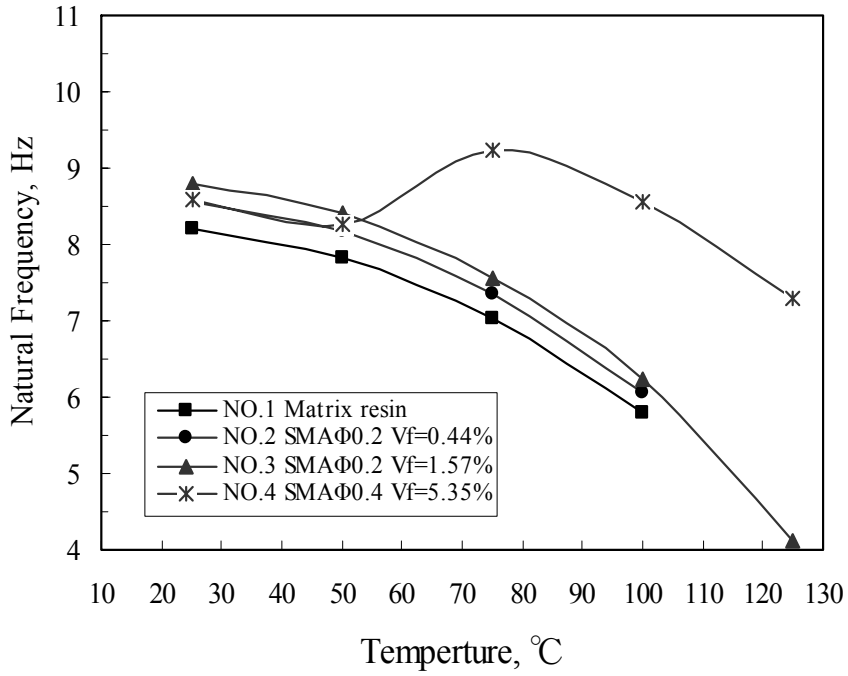
Natural Frequency, Hz
11
10
9
8
7
6
5
4
10 20 30 40 50 60 70 80 90 100 110 120 130
Temperture, ℃
NO.1 Matrix resin
NO.2 SMAΦ0.2 Vf=0.44%
NO.3 SMAΦ0.2 Vf=1.57%
NO.4 SMAΦ0.4 Vf=5.35%

Figure 12

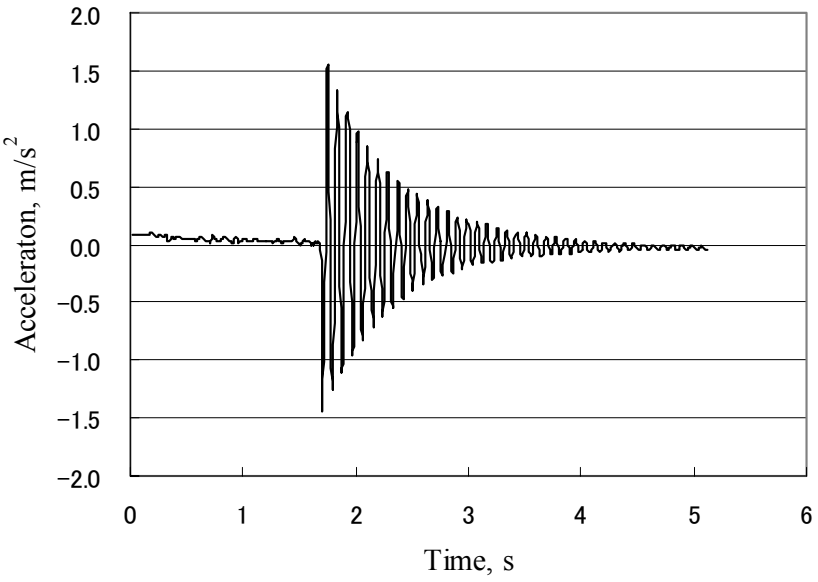

Figure 13

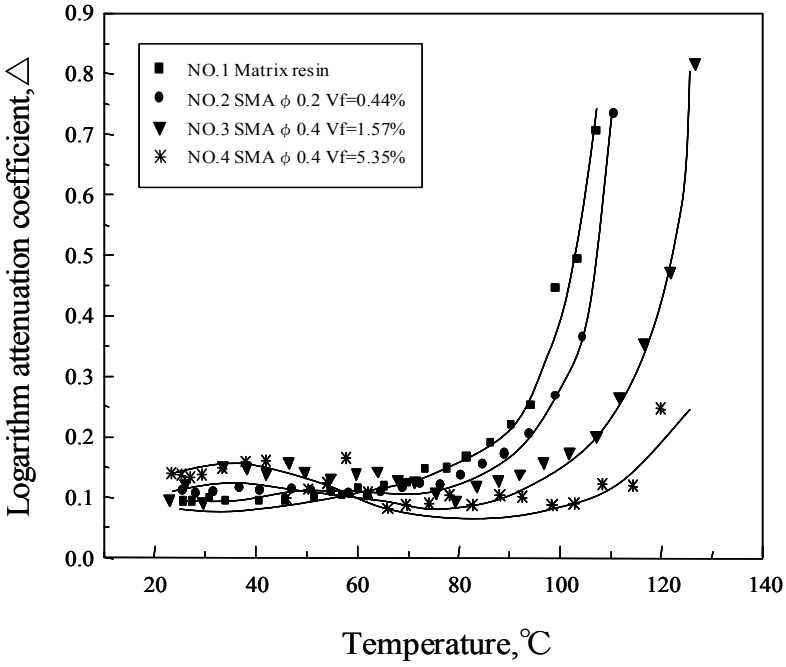
NO.1 Matrix resin
NO.2 SMA φ 0.2 Vf=0.44%
NO.3 SMA φ 0.4 Vf=1.57%
NO.4 SMA φ 0.4 Vf=5.35%
Logarithm attenuation coefficient,△
Temperature,℃
0.0
0.1
0.2
0.3
0.4
0.5
0.6
0.7
0.8
0.9
20
40
60
80
100
120
140

Figure 14

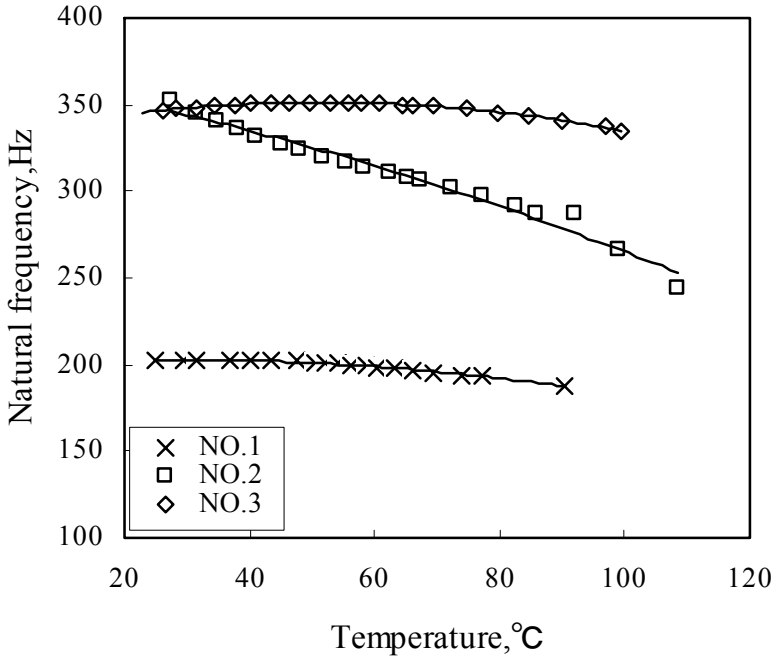
400
350
300
250
200
150
100
Natural frequency,Hz
NO.1
NO.2
NO.3
20
40
60
80
100
120
Temperature,℃

Figure 15

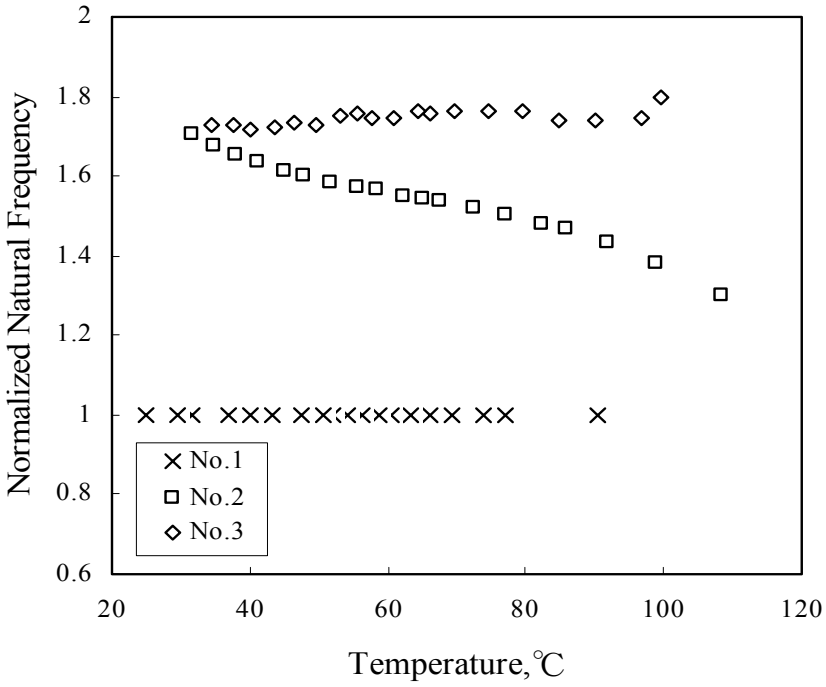
Normalized Natural Frequency
2
1.8
1.6
1.4
1.2
1
0.8
0.6
20
40
60
80
100
120
Temperature,℃
No.1
No.2
No.3

Figure 16

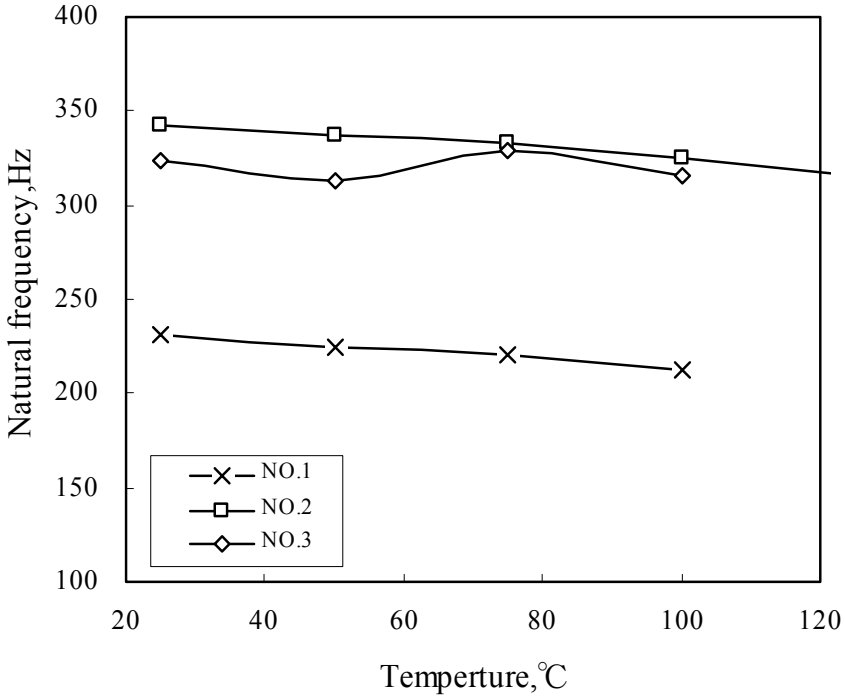
400
350
300
250
200
150
100
Natural frequency,Hz
20
40
60
80
100
120
Temperture,℃
NO.1
NO.2
NO.3

Figure 17

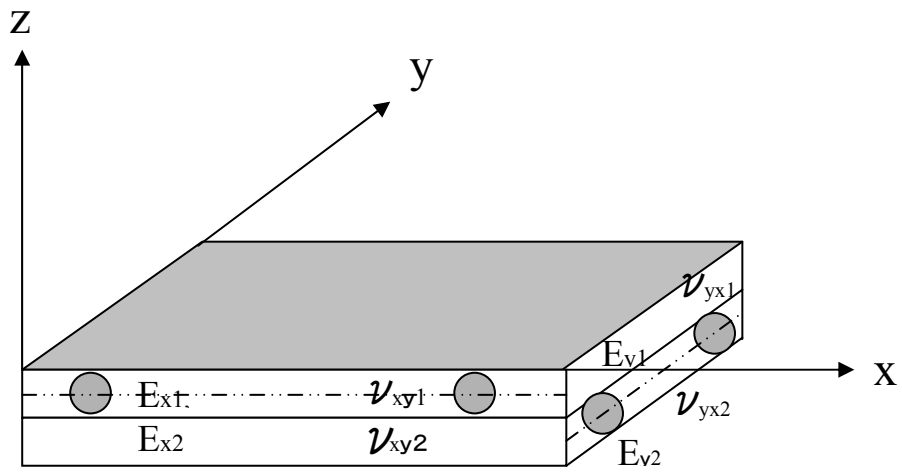

Table1 1

Materials	Elastic modulus *E* (GPa)	Poisson's ratio	ρ (kg/m^3)
SMA	20.4 ($T<A_s$) 71.4 ($T>A_f$)	0.30	6500
FRP	E_x : 12.9 E_y : 6.7	0.27	1161
Stainless steel	197.0	0.25	7800